


Damping Identification in Buildings from Earthquake Records

Conference Paper**Author(s):**

Bernal, Dionisio P.; [Mozaffari, Salma](#) ; Kwan, Kenny; Döhler, Michael

Publication date:

2012

Permanent link:

<https://doi.org/10.3929/ethz-b-000487919>

Rights / license:

[In Copyright - Non-Commercial Use Permitted](#)

Damping Identification in Buildings from Earthquake Records

D.Bernal¹, S. Mozaffari Kojidi¹, K. Kwan¹, M. Döhler¹

¹Civil and Environmental Engineering Department, Northeastern University, Center for Digital Signal Processing, Boston, MA

Abstract

It is shown that the Fisher information on damping contained in seismic response is small and, as a consequence, identified damping ratios are realizations from a distribution with high variance. Predictive expressions with reasonable confidence intervals can be generated, however, if sufficient data is available. In this study 122 responses from concrete buildings, 81 from steel, 26 for masonry and 10 from wood structures are used to identify damping ratios using a subspace algorithm. The regression expression derived for steel and concrete buildings is $\xi = a_0 + a_1 e^{-a_2 H}$, where H is the height, and for masonry and wood structures $\xi = (b_0 + b_1 e^{-b_2 S_A})^{-1}$, where S_A is the 5% damped Pseudo-Spectral acceleration. In these expressions a's and b's are coefficients.

Introduction

The term damping is used to refer to the collection of mechanisms by which systems dissipate energy. Although the inherent damping of structural systems is not viscous, velocity proportional dissipation is widely used because it leads to mathematical simplicity and because, at least for small damping, it can be calibrated to mimic the actual dissipation well. In practice it is customary to specify damping through modal damping ratios, defined as the quotient of the damping constant of the mode to the minimum value for which the response to arbitrary initial conditions does not have harmonic terms. The problem of extracting damping of viscously damped linear systems from input-output data is a standard problem in identification and exact results are obtained by all consistent algorithms when the data generating system satisfies the assumptions (Juang 1994, Verhaegen and Verdult 2007, Van Overschee and De Moor 1996, Heylen et al. 1997).

Notwithstanding the availability of theory, estimation of consistent damping values from measured response is difficult in structures subjected broadband excitation. The reason for this being the fact that the information (more precisely the Fisher information) about damping encoded in the response data is low. Low information implies that the estimated damping is a random variable with high variance and thus that realizations can differ substantially, either because the data set changes or because, for a given data set, details of the identification approach vary. One early example of discrepancies in damping estimates obtained for the same data set is that of the 12 high rise buildings subjected to the San Fernando earthquake, considered initially by Hart and Vasudevan (1975) and a few years later by McVerry (1979, 1980).

Predictors for damping ratios have been derived from the examination of data sets by various researchers. For example, Zhang and Cho (2009) extracted damping ratios from ambient vibration data for 82 buildings in Xi'an, China and proposed an expression for the first mode. Other studies include those by Jeary (1986), Lagomarsino (1993), Tamura et al. (1996), Sasaki et al. (1998) and Satake et al. (2003). In most previous studies where large data sets have been considered the vibration amplitudes have been very small and, as a consequence, the damping values obtained can be considered a lower bound. In this study we limited examination to responses where the peak ground acceleration was no less than 0.05g. The cases that satisfied this limit were 122 responses from concrete buildings, 81 from steel, 26 from masonry and 10 from wood structures. The theoretical base of the identification approach used to compute the damping values is summarized in Appendix A and the numerical values and the regressors for each considered case are presented in Appendix B.

Background and Relations

Equations of Motion

Let the subscript 1 stand for coordinates that are not prescribed and 2 for those that are. The equations of motion of a viscously damped linear system without external excitations can then be written as

$$\begin{bmatrix} M_{11} & M_{12} \\ M_{21} & M_{22} \end{bmatrix} \begin{Bmatrix} \ddot{y}_1 \\ \ddot{y}_2 \end{Bmatrix} + \begin{bmatrix} C_{11} & C_{12} \\ C_{21} & C_{22} \end{bmatrix} \begin{Bmatrix} \dot{y}_1 \\ \dot{y}_2 \end{Bmatrix} + \begin{bmatrix} K_{11} & K_{12} \\ K_{21} & K_{22} \end{bmatrix} \begin{Bmatrix} y_1 \\ y_2 \end{Bmatrix} = \begin{Bmatrix} 0 \\ R_e \end{Bmatrix} \quad (1)$$

where R_e are the reactions at the prescribed coordinates. The displacements that are not prescribed can be expressed as a linear combination of the prescribed ones plus a residual, namely

$$y_1 = ry_2 + u \quad (2)$$

which, when substituted into the top partition of eq.1 gives

$$M_{11}\ddot{u} + C_{11}\dot{u} + K_{11}u = -(M_{12} + M_{11}r)\ddot{y}_2 - (C_{12} + C_{11}r)\dot{y}_2 - (K_{12} + K_{11}r)y_2 \quad (3)$$

Since the matrix r is arbitrary, it can be selected to cancel any of the terms on the *rhs* of eq.3, taking r as

$$r = -K_{11}^{-1}K_{12} \quad (4)$$

neglecting the damping contribution to the *rhs* term, and recognizing that for lumped mass models one has $M_{12} = 0$, one gets

$$M_{11}\ddot{u} + C_{11}\dot{u} + K_{11}u = -M_{11}r \ddot{y}_2 \quad (5)$$

which is the conventional expression used to represent earthquake excitation. The point to note here is that the properties on the matrices on the *lhs* of eq.5 are those of the system with restraints

at the prescribed coordinates. This means that if only horizontal motion is used to define the input, the properties that a system identification algorithm obtains include the flexibility and dissipation at the soil structure interface in all DOF other than horizontal translation. For familiarity in the subsequent treatment we drop the subscripts in eq.5 and replace \ddot{y}_2 by the more commonly used \ddot{x}_g , namely, we use

$$M \ddot{u} + C \dot{u} + K u = -M r \ddot{x}_g \quad (6)$$

Damping Ratio

Let the *rhs* of eq.6 equal zero, namely

$$M \ddot{u} + C \dot{u} + K u = 0 \quad (7)$$

the solution to eq.7 is of the form $u(t) = \sum \alpha_i \psi_i e^{s_i t}$ and one finds, by substitution that

$$\left[M s_i^2 + C s_i + K \right] \psi_i = 0 \quad (8)$$

where α_i 's are scalars. The values of s_i 's that satisfy the equation are complex and come in complex conjugate pairs. Writing the solution in terms of its real and its imaginary part, calling on Euler's identity, and replacing s by the value at the solution, λ , one finds that

$$u(t) = \sum \alpha_i \psi_i e^{\lambda_{iR} t} (\cos(\lambda_{iI} t) + i \sin(\lambda_{iI} t)) \quad (9)$$

which shows that the rate of decay of the free vibration is determined by the real part of the eigenvalue and the vibration frequency by the imaginary. The definition of damping ratio, which does not require that the damping be classically distributed, is

$$\xi = \frac{-\lambda_R}{|\lambda|} \quad (10)$$

Eq.10 allows for a simple appreciation of why it is difficult to identify damping ratios with low variance. Namely, let the true pole for a given mode be a point in the complex plane and let there be a region around the pole where, due to noise, the identification algorithm places the pole. Assume the region of uncertainty around the pole is a circle of radius R , where R is a fraction of the pole magnitude, say $R = \alpha |\lambda|$. Noting that the magnitude of the pole is an estimate of the undamped frequency (exact for classical damping) and recognizing that α is small, one concludes that the variability in frequency is small. The estimation of damping, however, which is given by eq.10, can experience much larger variations. In fact, examination of the geometry shows that the percent error in the frequency is essentially equal to α while the damping ratio ranges from the true value to plus or minus α . Let α be 0.02, for example, in this case the frequency error is no more than 2% but the damping ratio can be over or under estimated by 0.02. If the true damping is 5%, for example, one gets values as large as 7% and as low as 3%. To determine if the circular assumption for the uncertainty region is reasonable, we carried out a Monte Carlo study where a system was identified 1000 times using random realizations of the

noise. As can be seen from fig.1, which shows results for the first and the second pole, the circular premise is not unreasonable.

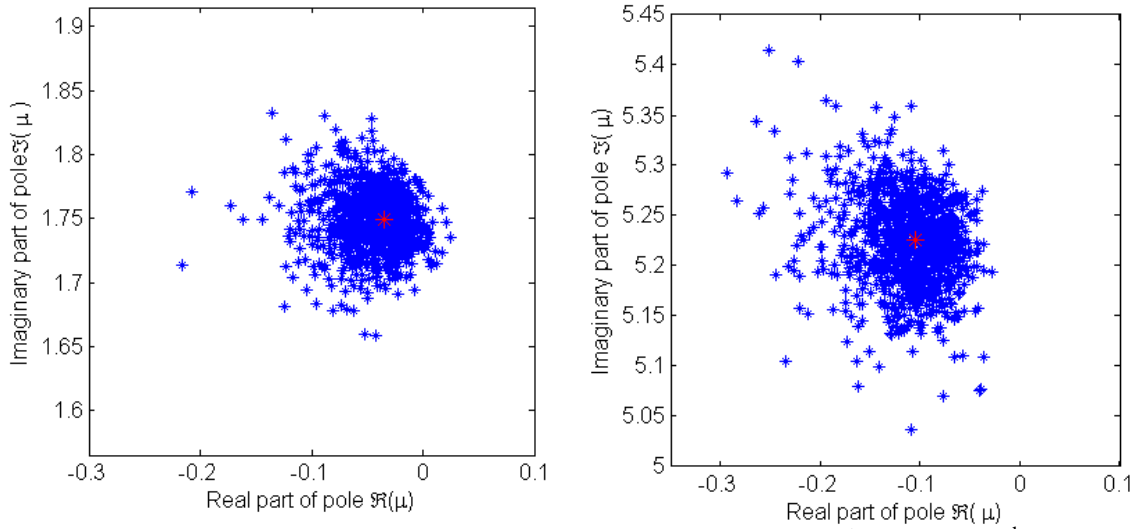


Figure 1. Uncertainty of the real part vs. the imaginary part of the 1st pole and 2nd pole in a 10-DOF system identified using white excitation and 5% additive noise.

Some Proposed Damping Predictors

Predictors for damping in buildings have been proposed through the years and some are summarized next:

Table 1. Damping Predictors

Expression	Source
$\zeta_1 = 0.01f_1 + 10^{\sqrt{D}/2} x / H$	Jeary (1986)
$\zeta_1 = 0.013f_1$ (Steel) $\zeta_1 = 0.014f_1$ (RC)	Satake et al. (2003)
$\zeta_1 = 1.945 + 0.195T_1^{-3.779}$	Zhang and Cho (2009)
$\zeta_1 = 0.013f_1 + 0.0029$ (Steel)	Sasaki (1998)
$\zeta_1 = 0.014f_1 + 470 \frac{x}{H} - 0.0018$ (Steel) $\zeta_1 = 0.013f_1 + 470 \frac{x}{H} + 0.0029$ (RC)	Satake (2003)
$\zeta_1 = \frac{\alpha}{f_1} + \beta f_1 + \gamma \left(\frac{x}{H} \right)$ $\alpha = 0.0072, \beta = 0.0070$ (RC) $\alpha = 0.0032, \beta = 0.0078$ (Steel)	Lagomarsino (1993)
For higher modes damping ratios: $\zeta_n = (1.3 \sim 1.4)h_{n-1}$ (Steel) $\zeta_n = 1.4h_{n-1}$ (RC) $\zeta_n = (1.7 \sim 1.8)h_{n-1}$ (SRC)	Satake et al. (2003)

Discussion

The expressions in Table 1 show that the damping ratio tends to increase with frequency and, although only noted in some of the expressions, also with amplitude. Justification for correlation with amplitude is evident but the rationale for the correlation with frequency is less apparent. In this regard it is possible that the causal connection is not with frequency per se but with some measure of the size of the interface between the structure and the ground, a possible explanation being that the larger the interface the larger the energy dissipation that can take place through this interface. Another item worth commenting on is the issue of how the damping ratios in higher modes compare to that of the first mode. In particular, Satake et al., (2003) has postulated, based on a trend observed in the first few modes, that the expected value of the damping ratio is higher in the modes above the fundamental. Examination suggests that this observation may derive from the effectiveness of the mode shape in activating the dissipation mechanism. To illustrate, consider a 6-story one bay model where the damping is assumed to come from dashpots of equal magnitude located at each of the connections between beams and columns. The damping ratio when behavior is dominated by frame action (relatively rigid beams) and where flexure dominates (relatively flexible beams) is depicted in fig.2. As can be seen, the damping increases in the early modes but eventually decreases, as the joint rotations for sufficiently high modes are small. The results for the shear type behavior are (in this case at least) in qualitative agreement with the ratios proposed by Satake for increases from the 1st to 2nd and the 2nd to 3rd mode.

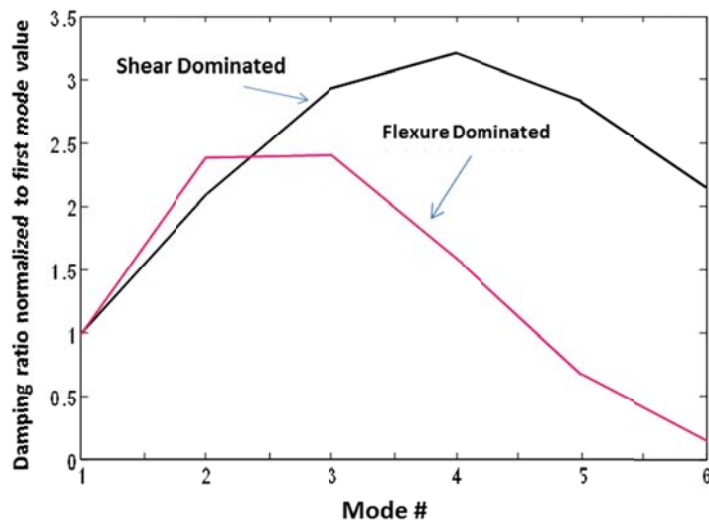


Figure 2. Ratio of damping between various modes in a 6-story model with dissipation simulated with dashpots at the beam-column joints.

Sensitivity of Identified Damping to Nonlinear Response

Although the data in this study does not include cases with large yielding it is of interest to note that the increases in effective damping due to modest yielding are not as large as one may anticipate at first glance, the reason being the short duration of the response over which the

nonlinearity is activated. To illustrate, the identified frequencies and equivalent damping of a SDOF with a frequency of 1 Hz and 5% viscous damping were obtained from identification for three different response levels using the Whittier ground motion. The first level is linear and is used to confirm that the ID is able to identify the correct model. The other two correspond to nominal displacement ductility levels of 2 and 4. The identified damping values are {5, 5.82, and 8.4} percent and the identified frequencies are {1, 0.99, and 0.98} hertz respectively. Plots of the resulting force vs. drift are depicted in fig.3.

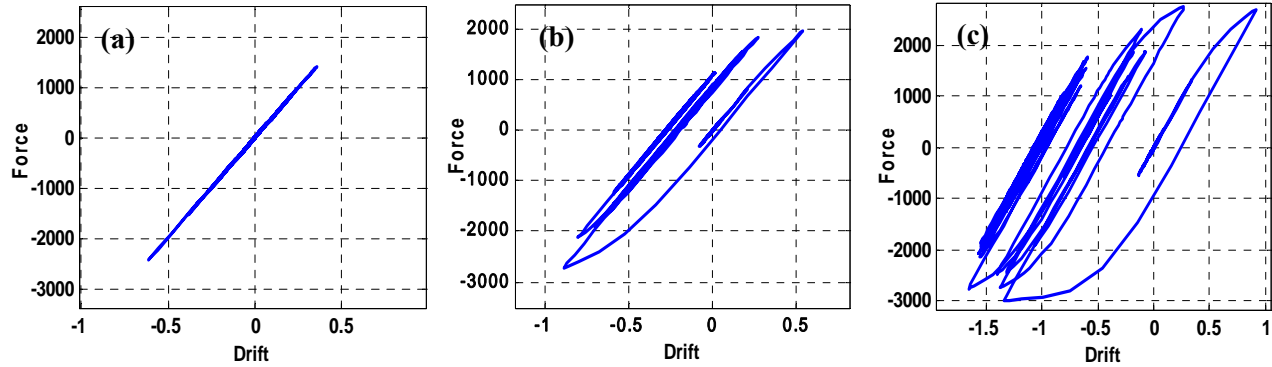


Figure 3. Force vs. drift for three response levels (a)-(c)

Uncertainty in Damping Estimation

This section presents some discussion on the estimation of damping from the perspective of the “information content” of a parameter in available data. It is shown that for conditions that are typical the coefficient of variation of damping ratios can be more than 50 times higher than that of frequencies. Similar results on the identification of ARMA models have been reported in Gersch (1974).

The Cramér-Rao Lower Bound and the Fisher Information

The accuracy with which any parameter can be estimated from noisy data is limited by the amount of information on the parameter that is contained in the data. For any distribution of the noise affecting the input and the output, the lower bound to the covariance Σ that a parameter estimator can have is known as the *Cramér-Rao Lower Bound* (CRLB) (Casella and Berger 2001). The CRLB depends only on the statistical distribution of the noise and on the sensitivity of the data to the parameter. The inverse of the CRLB is known as the *Fisher Information* (FI), which indicates “how much information” on the parameter is contained in the data set. Technically, the FI is defined as

$$I(\theta) = \mathbf{E} \left(\frac{\partial}{\partial \theta} \log f(Y | \theta) \right)^2 \quad (11)$$

where $f(Y | \theta)$ is the probability density function of the observed data Y given the parameter θ . If the sensitivity of the likelihood to the parameter is high the derivative in eq.11 is large and so

is $I(\theta)$. In practice, the likelihood function $f(Y|\theta)$ is in general unknown so other quantities derived from the data are used. For example, if the data can be used to generate a vector X that is normally distributed having a mean that depends on the parameters, $\gamma(\theta)$, and a covariance Σ , the FI of the parameter θ contained in X can be obtained as (van den Bos 2007)

$$I(\theta) = \mathcal{J}(\theta)^T \Sigma^{-1} \mathcal{J}(\theta) \quad \text{where} \quad \mathcal{J}(\theta) = \frac{\partial \gamma}{\partial \theta}. \quad (12)$$

Denoting Σ_λ as the covariance of the real and imaginary part of a pole, the FI of the frequency and the damping follows from eq.12 as

$$I(\xi, f) = \mathcal{J}_{\xi, f}^T \Sigma_\lambda^{-1} \mathcal{J}_{\xi, f} \quad (13)$$

where the sensitivity of the pole with respect to damping ratio and frequency is given by

$$\mathcal{J}_{\xi, f} = \frac{\partial(\Re(\lambda), \Im(\lambda))}{\partial(\xi, f)} = 2\pi \begin{bmatrix} -f & -\xi \\ -f\xi(1-\xi^2)^{\frac{1}{2}} & \sqrt{1-\xi^2} \end{bmatrix}. \quad (14)$$

Due to the relation between the FI and the CRLB, an analytical relationship between the coefficients of variation of damping and frequency can be obtained from eq.14. This relation shows that the ratio depends only on the damping ratio. Assuming that the uncertainty region around the complex poles is circular, as depicted in the Monte-Carlo simulation in fig.1, the ratios between the coefficients of variation are shown in fig.4. As can be seen, the uncertainty on the damping ratios is around 50 times higher than that for the frequencies at $\xi = 0.02$, and the ratio is near 25 for $\xi = 0.05$.

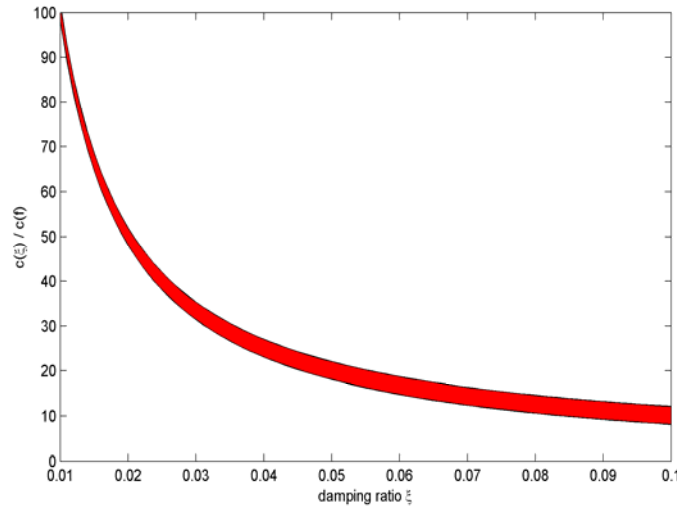


Figure 4. Range of the ratio of the coefficient of variation of damping and frequency when the uncertainty region around the pole is circular

Regression Analysis

The regressors considered here are the peak ground motion parameters (PGA, PGV and PGD), the spectral ordinates (SA, SV and SD), the building height, H, the frequency of the mode, f, and the effective duration $t_{0.9}$. This last entry defined as the time interval between the attainment of 5% and 95% of the total integral of the acceleration squared. Examination of the effect of duration on the variance of identified damping showed that the standard deviation varies inversely with the square root of the duration normalized by the modal period. This result was used in the regression to normalize the residuals to equal variance.

Goodness of Fit

When measurements have significant variance the goodness of fit cannot be judged from a simple inspection of the scatter. The standard goodness of fit test is the F-test for lack of fit (FTLF). The test operates with residuals of equal variance, which in our case are given by

$$\hat{r}_i = (\xi_i - \xi_{p,i}) \sqrt{\Omega_i \cdot t_{0.9,i}} \quad (15)$$

and

$$\hat{d}_i = (\xi_i - \bar{\xi}_i) \sqrt{\Omega_i \cdot t_{0.9,i}} \quad (16)$$

from where the F statistic is computed as

$$F = \frac{\sum_{j=1}^n \left(\sum_{i=1}^{n_i} \frac{\hat{r}_{i,j}}{\sqrt{n_i}} \right)^2 \cdot \frac{1}{(n-p)}}{\sum_{j=1}^n \left(\sum_{i=1}^{n_i} \hat{d}_{i,j} \right)^2 \cdot \frac{1}{(N-n)}} \quad (17)$$

where n = number of bins, n_i = number of samples in the i^{th} bin, N = total number of observations, ξ_i = data point, $\xi_{p,i}$ = predicted value and $\bar{\xi}_i$ = mean of the data points in a bin. Bins are such that the prediction varies little within the bin (5% of the average in our numerical results). The F statistic has a Fisher-Snedecor distribution with $(n-p)$ and $(N-n)$ degrees of freedom for the numerator and the denominator and a low value indicates a good fit. Results on the goodness of fit, however, are most easily interpreted in terms of the p-value of the F statistic. The p-value is such that if it is smaller than the acceptable Type I error rate the proposed fit is rejected. The Type I error, in this case, consists in rejecting the proposed fit when it is valid one. The typical p-value threshold is 0.05.

Coefficient of Determination

The coefficient of determination, R^2 , defined as

$$R^2 = 1 - \frac{\sum_i (y_i - y_{p,i})^2}{\sum_i (y_i - \bar{y})^2} \quad (18)$$

is widely used in diagnosing regression results. The coefficient is essentially a measure of how much the regression line reduces the scatter relatively to the mean. Low values of R^2 , however, do not invalidate regression results when the intrinsic variance of the data is large.

Functional Form

We considered a number of different forms and settled on two exponential ones: one for cases where the damping decreases and the other for cases where the damping increases with the regressor, namely;

$$\hat{\xi} = a_0 + a_1 e^{-a_2 \theta} \quad (19a)$$

and

$$\hat{\xi} = \frac{a_0}{1 + a_1 e^{-a_2 \theta}} \quad (19b)$$

Results

The regression was carried out for the first mode damping ratio for steel, concrete, masonry, and wood buildings. When the mode considered is dominated by translation in one direction the ground motion in this direction was used to compute the ground motion parameters. When the mode is strongly coupled, or torsional, the average of the ground motion parameters for the two directions was used. The best results for the expected value of the first mode damping ratio are:

$$\xi_s = 1.22 + 4.26 e^{-0.013H} \quad (\text{steel}) \quad (20)$$

$$\xi_c = 2.91 + 3.54 e^{-0.018H} \quad (\text{concrete}) \quad (21)$$

$$\xi_m = \frac{1}{0.11 + 0.23 e^{-8.84 S_A}} \quad (\text{masonry}) \quad (22)$$

$$\xi_w = \frac{1}{0.09 + 0.17 e^{-3.37 S_A}} \quad (\text{wood}) \quad (23)$$

where H is in meters and S_A is the 5% pseudo-spectral acceleration in g 's. Plots of the regression, the 95% confidence intervals, and the data, are presented in figs5-8.

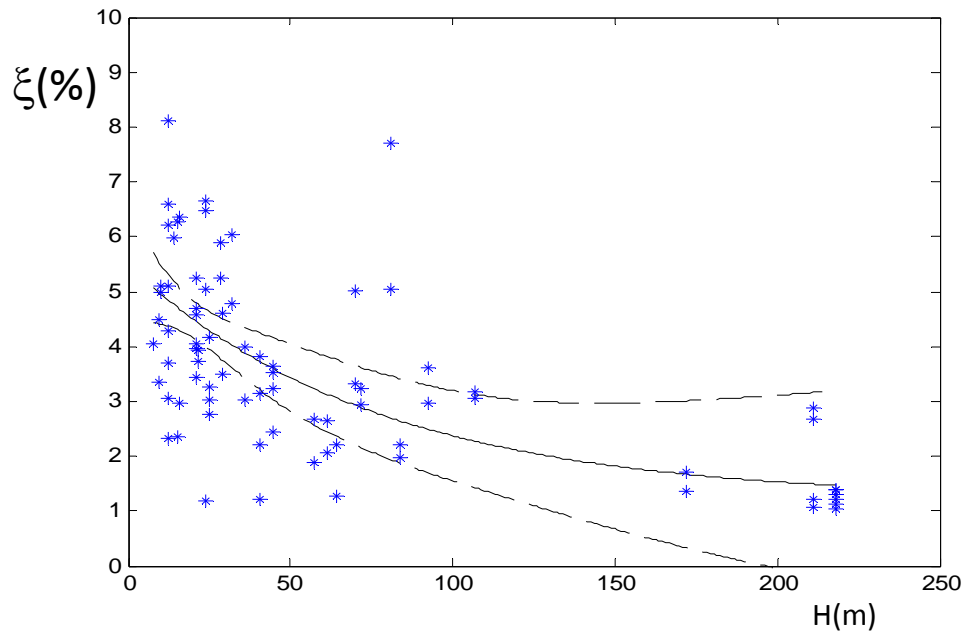


Fig.5 Regression result (steel buildings) and 95% confidence limits, $R^2=0.37$, F-test p-value = 0.85

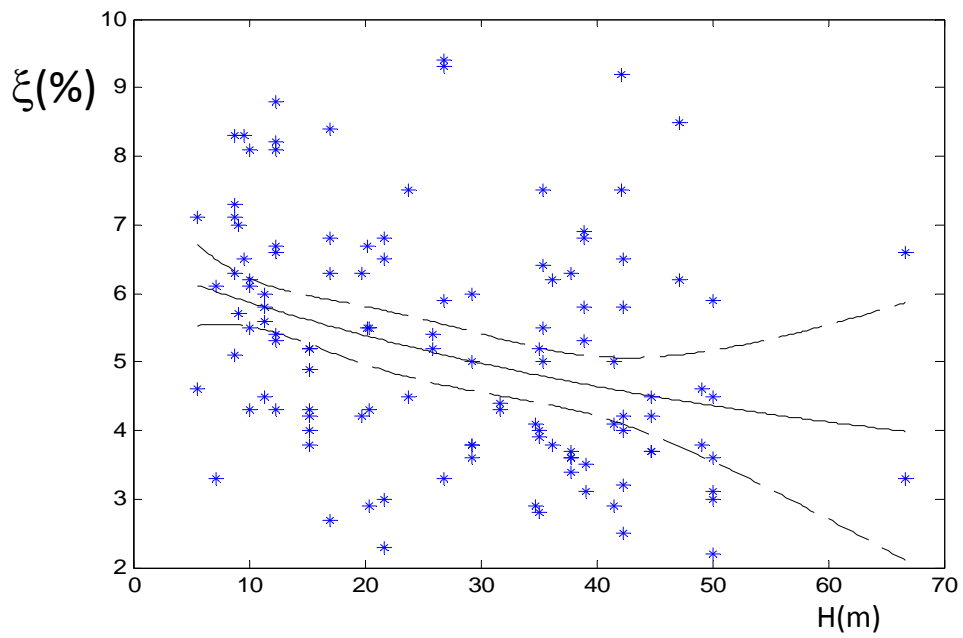


Fig.6 Regression result (concrete buildings) and 95% confidence limits, $R^2=0.11$, F-test p-value=0.72

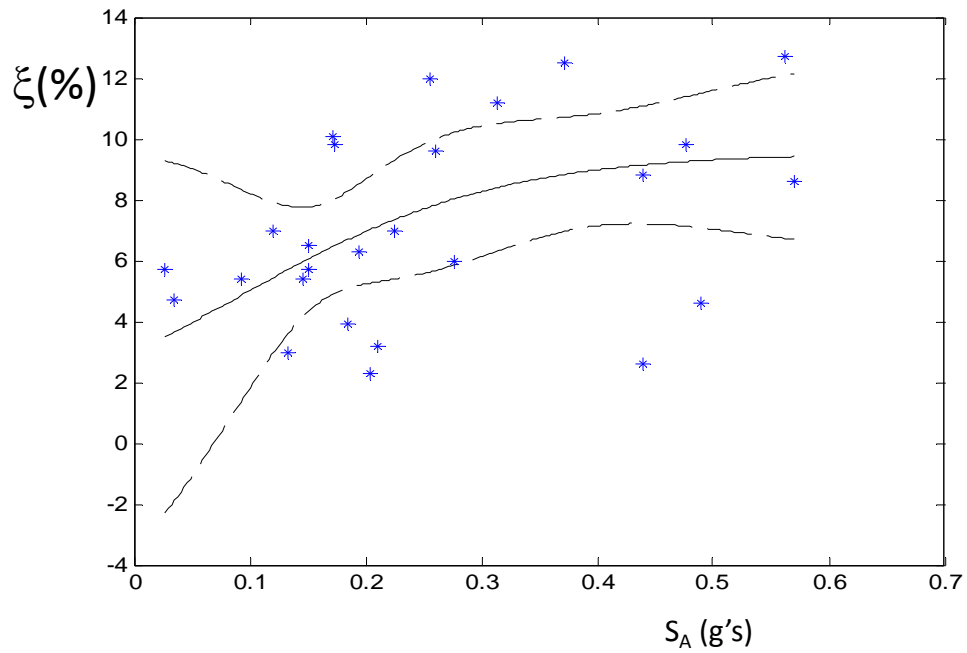


Fig.7 Regression result (masonry buildings) and 95% confidence limits, $R^2=0.15$, F-test p-value =0.25

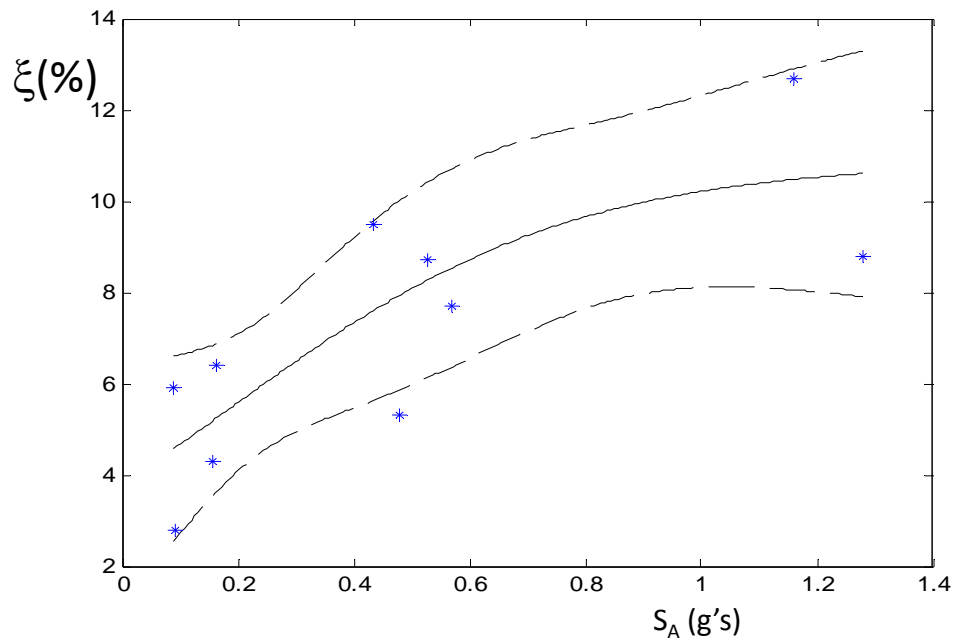


Fig.8 Regression result (wood buildings) and 95% confidence limits, $R^2=0.64$, F-test p-value =0.97

Discussion

For steel buildings H provided the best correlation with damping ratio by a significant margin. In concrete buildings the expression based on S_A produced results that are only slightly less correlated than those for H . For masonry and wood buildings the correlation with S_A was clearly the superior choice. These results are along the line of what one expects from qualitative reasoning. Namely, in steel most of the intensity related increase in damping (in the linear range) is related to non-structural components while in the other structural types there is also a lateral load resisting mechanism dependence. For completeness, figs.9 and 10 show the correlation of damping ratio with S_A for steel and concrete buildings. The fact that dependence on S_A saturates very quickly in steel and less so in concrete is evident from the plots and from the coefficient in front of S_A in the best fit expressions.

A question that comes to mind is whether a multivariate regression using both H and S_A could lead to notable improvements but the answer to this proved negative because the two parameters happen to be correlated. It is not difficult to see that this is so because as the height increases the period lengthens and the spectral accelerations, except for short buildings, decrease. For the buildings considered here the correlation coefficients between H and S_A are -0.57 and -0.39 for steel and concrete, respectively.

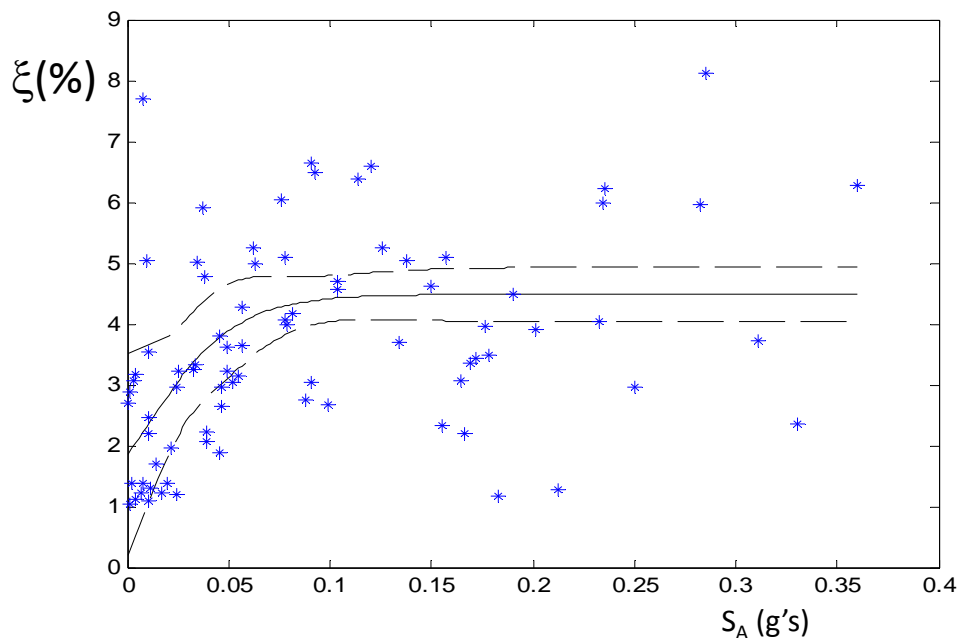


Fig.9 Regression with 5% damped pseudo spectral acceleration (steel buildings) and 95% confidence limits, $R^2=0.15$, F-test p-value =0.25

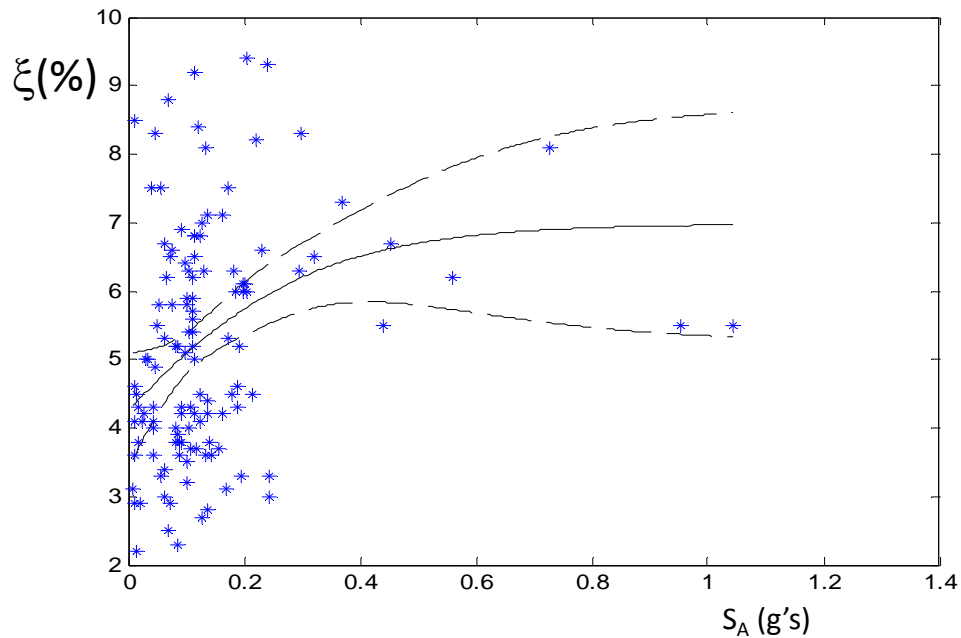


Fig.10 Regression with 5% pseudo-spectral acceleration (concrete buildings) and 95% confidence limits, $R^2=0.64$, F-test p-value =0.97

A final item worthy of attention is whether or not there is consistency in the results of the regression for damping as a function of H and SA. Examination shows that the results are indeed consistent. To clarify consider these two situations: a) say a steel building has $H = 50$ m. From the plot in fig.5 one finds that the 95% confidence for the regression is from 2.8% to 4.05%. Looking at fig.9 one finds that this could be the solution for any value of SA, b) consider $H = 200$ m. In this case the 95% confidence interval is from 0 to 3%. Looking at fig.9 one concludes that consistency requires that SA for this building be no larger than 0.047 g. The data shows that there are 28 records for buildings whose heights are 200 m or more and that, of all these, there are only two cases where SA exceeded this limit. This small violation is, of course, reasonable since a 95% confidence interval does not provide complete certainty.

Conclusions

It is shown that damping ratios identified from earthquake records are realizations from distributions with high variance. The reason for the high variance is traced to the low sensitivity of the transient response to damping and it can be visualized from the pole location in the complex plane and the distribution of the uncertainty. The paper shows that the coefficient of variation of damping estimates are 25 to 50 times larger than the coefficient of variation of frequency estimates. The large variance does not preclude, however, estimation of reasonable values for the damping ratio when sufficient data is available. For steel and concrete buildings there are 122 and 81 points, respectively, and, as a consequence, results for the 95% confidence intervals of the expectation are significantly tighter than the deviation inherent in the identified results. For masonry the confidence interval opens up notably since there are only 27 points and finally, for wood, where there are only 10 data points, the confidence interval contains

essentially all of the data. The expressions proposed to estimate the first mode damping ratio are slightly more complex than linear but offer the advantage of having asymptotic behavior so there is no need to impose arbitrary limits to avoid negative damping or unreasonably large values. The results show that damping in steel buildings is, except for very tall buildings, larger than the 2% that is typically assigned in practice. The expected value of damping in masonry structures is higher than for concrete and wood structures display damping values somewhat higher than those of masonry.

Acknowledgements

The research reported in this paper was carried out with support from the California Strong Motion Instrumentation Program (CSMIP) through standard agreement 1010-934. This support is gratefully acknowledged.

Appendix A – Identification

Time domain algorithms are typically based on an indirect approach. Namely, a model mapping the sampled input and the sampled output is obtained and then it is converted to continuous time. The postulated model in sampled time has the form

$$x(k+1) = A_d x(k) + B_d \ddot{x}_g(k) \quad (\text{a.1})$$

where the measurements are given by

$$\ddot{y}(k) = Cx(k) \quad (\text{a.2})$$

The procedure begins by noting that for the model in eq.a.1 the output is related to the input as

$$y(k) = \sum_{j=1}^k Y_j \ddot{x}_g(k-j) \quad (\text{a.3})$$

where Y_j , known as a Markov Parameter (MP) is given by

$$Y_j = CA_d^{j-1} B_d \quad (\text{a.4})$$

Once the MP are obtained from eq.a.3, the next task is to untangle the matrices $\{A_d, B_d, C\}$ from the triple product. This is done by defining the Hankel matrix H_k as

$$H_k = \begin{bmatrix} Y_{k+1} & Y_{k+2} & \cdots & Y_{k+\beta} \\ Y_{k+2} & Y_{k+3} & \cdots & Y_{k+\beta} \\ \vdots & \vdots & \vdots & \vdots \\ Y_{k+\alpha} & \cdot & \cdots & Y_{k+\beta+\alpha-1} \end{bmatrix} \quad (\text{a.5})$$

where α and β are user defined parameters and noting that with

$$P_\alpha = \begin{bmatrix} C_d \\ C_d A_d \\ \vdots \\ C_d A_d^{\alpha-1} \end{bmatrix} \quad (\text{a.6})$$

and

$$Q_\beta = [B_d \quad A_d B_d \quad A_d^2 B_d \quad \cdots \quad A_d^{\beta-1} B_d] \quad (\text{a.7})$$

$$H_k = P_\alpha A_d^k Q_\beta \quad (\text{a.8})$$

so it follows that H_0

$$H_0 = P_\alpha Q_\beta \quad (\text{a.9})$$

one then performs a singular value decomposition of H_0 , namely

$$H_0 = R \Sigma S^T \quad (\text{a.10})$$

and after retaining only the N most important singular values, has

$$H_0 = R_N \Sigma_N S_N^T \quad (\text{a.11})$$

where R_N contains the first N columns of R , S_N the first N columns of S and Σ_N is the diagonal matrix having the N significant singular values. Splitting the diagonal singular value matrix into the product of two matrices (E_1 and E_2)

$$E_1 E_2 = \Sigma_N \quad (\text{a.12})$$

gives

$$H_0 = (R_N E_1)(E_2 S_N^T) \quad (\text{a.13})$$

and one can then take

$$P_\alpha = R_N E_1 \quad (\text{a.14})$$

$$Q_\beta = E_2 S_N^T \quad (\text{a.15})$$

from where, given the definitions in eq.'s a.6 and a.7 one has that

- The first m rows of P_α provide a realization for C .
- The first r columns of Q_β provide a realization for B_d .

The matrix A_d can be obtained from the block Hankel matrix for $k = 1$, namely, given that

$$H_1 = P_\alpha A_d Q_\beta = R_N E_1 A_d E_2 S_N^T \quad (\text{a.16})$$

and the fact that R_N and S_N are orthonormal one gets

$$A_d = E_1^{-1} R_N^T H_1 S_N E_2^{-1} \quad (\text{a.17})$$

Discrete to Continuous Transfer

Once the sampled time model is available its conversion to continuous time follows as (Bernal 2006)

$$A_c = \frac{1}{\Delta t} \ln(A_d) \quad (\text{a.18})$$

$$B_c = \frac{1}{\Delta t} A_d^{-1} B_d \quad (\text{a.19})$$

$$C_c = C \quad (\text{a.20})$$

The damping ratios are obtained as the real part of the eigenvalues of A_c divided by their magnitude.

Appendix B - Data

Table B.1. Data Used in the Regression Analysis

Station #	Earthquake	f_1 (Hz)	ζ_1 (%)	H(m)	S_A (g)	S_V (cm/s)	S_D (cm)	PGA(g)	PGV(cm/s)	PGD(cm)	$t_{0.9}$ (s)
58496	LomaPrieta	3.08	4.0	7.7	0.233	11.8	0.6	0.12	7.3	1.1	11.2
24198	Chinohills	1.46	5.1	10.4	0.077	8.3	0.9	0.07	5.8	0.6	19.3
24198	Chinohills	1.52	5.0	10.4	0.063	6.4	0.7	0.04	3.5	0.5	21.9
54331	MammothLakes	3.56	3.4	9.7	0.169	7.4	0.3	0.12	3.9	0.2	4.0
54331	MammothLakes	5.85	4.5	9.7	0.190	5.1	0.1	0.12	4.2	0.2	3.9
58506	LomaPrieta	1.41	6.0	14.1	0.282	31.2	3.5	0.11	20.3	4.7	20.9
58506	LomaPrieta	1.59	6.0	14.1	0.234	23.0	2.3	0.08	12.9	3.2	22.0
23516	Landers	1.65	6.2	12.6	0.236	22.3	2.2	0.08	15.1	7.6	38.6
23516	Landers	1.83	8.1	12.6	0.286	24.3	2.1	0.11	23.8	12.6	34.3
23516	Chinohills	1.65	2.3	12.6	0.155	14.7	1.4	0.07	4.8	0.4	38.7
23516	Chinohills	2.07	3.1	12.6	0.164	12.4	1.0	0.07	4.8	0.4	38.7
23516	SanBernardino	1.73	6.6	12.6	0.120	10.9	1.0	0.10	7.3	0.5	5.5
23516	SanBernardino	1.99	4.3	12.6	0.057	4.5	0.4	0.08	2.6	0.2	7.7
57562	LomaPrieta	1.39	2.3	15.1	0.330	37.1	4.3	0.18	17.5	5.5	10.1
57562	LomaPrieta	1.49	6.3	15.1	0.360	37.7	4.0	0.20	15.4	3.3	10.5
24104	Chatsworth	1.96	3.7	12.5	0.134	10.7	0.9	0.08	6.1	0.4	4.5
24104	Chatsworth	2.26	5.1	12.5	0.157	10.9	0.8	0.07	5.1	0.4	6.8
24370	Whittier	0.78	2.8	25.2	0.088	17.7	3.6	0.23	12.5	1.3	6.9
24370	Whittier	0.81	4.2	25.2	0.081	15.7	3.1	0.17	9.7	1.2	7.8
24370	SierraMadre	0.78	3.0	25.2	0.052	10.4	2.1	0.12	5.8	0.8	9.7
24370	SierraMadre	0.81	3.3	25.2	0.033	6.3	1.2	0.11	7.9	0.8	8.0
24609	Landers	1.32	5.1	23.9	0.138	16.2	2.0	0.08	10.4	5.1	40.2
24609	Landers	1.47	6.5	23.9	0.092	9.8	1.1	0.05	8.6	4.9	46.9
24609	Northridge	1.32	6.6	23.9	0.091	10.8	1.3	0.06	8.9	2.7	25.6
24609	Northridge	1.49	1.2	23.9	0.183	19.2	2.0	0.07	8.0	2.6	27.3
14323	Whittier	0.72	4.8	31.7	0.039	8.4	1.9	0.06	6.5	0.9	25.4
14323	Whittier	0.88	6.0	31.7	0.076	13.5	2.4	0.04	4.4	0.5	26.6
24652	Northridge	0.98	3.9	21.8	0.202	32.2	5.2	0.20	14.0	3.1	19.2
24652	Northridge	1.46	3.7	21.8	0.311	33.3	3.6	0.20	14.0	3.1	19.2
23481	Landers	0.64	5.9	28.8	0.038	9.2	2.3	0.06	5.9	2.3	27.5
23481	Landers	0.71	5.3	28.8	0.062	13.7	3.1	0.07	6.5	2.4	26.4
23515	Landers	0.48	4.0	35.9	0.078	25.6	8.5	0.07	14.8	5.4	41.2
23515	Landers	0.50	3.0	35.9	0.091	28.6	9.1	0.09	15.0	7.5	40.5
23634	BigBear	2.02	4.7	21.0	0.104	8.0	0.6	0.06	5.0	1.5	32.1
23634	BigBear	2.40	5.2	21.0	0.126	8.2	0.5	0.06	5.0	1.5	32.1
23634	Landers	2.00	4.0	21.0	0.176	13.8	1.1	0.08	12.4	6.5	40.4
23634	Landers	2.07	3.4	21.0	0.172	12.9	1.0	0.08	12.4	6.5	40.4

Station #	Earthquake	f_1 (Hz)	ζ_1 (%)	H(m)	S_A (g)	S_V (cm/s)	S_D (cm)	PGA(g)	PGV(cm/s)	PGD(cm)	$t_{0.9}$ (s)
23634	Northridge	2.04	4.6	21.0	0.104	8.0	0.6	0.05	4.3	0.7	31.0
23634	Northridge	2.07	4.1	21.0	0.078	5.9	0.5	0.06	4.3	0.9	29.3
24248	Chinohills	1.45	3.7	44.8	0.056	6.1	0.7	0.05	2.7	0.3	19.7
24248	Chinohills	1.49	3.2	44.8	0.050	5.2	0.6	0.05	3.2	0.5	20.3
24248	WhittierNarrows	1.55	3.5	44.8	0.010	1.0	0.1	0.05	1.2	0.1	5.4
24248	WhittierNarrows	1.60	2.5	44.8	0.010	1.0	0.1	0.05	1.3	0.1	5.0
24249	Chinohills	1.40	3.1	40.9	0.055	6.1	0.7	0.07	3.3	0.5	15.9
24249	Chinohills	1.44	3.8	40.9	0.045	4.9	0.5	0.08	3.7	0.7	15.2
24249	WhittierNarrows	1.47	2.2	40.9	0.010	1.1	0.1	0.05	1.5	0.1	5.9
24249	WhittierNarrows	2.06	1.2	40.9	0.025	1.9	0.1	0.05	1.5	0.1	5.9
24514	Whittier	2.87	3.5	29.3	0.178	9.7	0.5	0.06	3.7	0.6	14.0
24514	Whittier	3.32	4.6	29.3	0.150	7.0	0.3	0.05	3.4	0.5	14.2
58261	LomaPrieta	1.21	6.4	16.0	0.114	14.7	1.9	0.06	8.8	2.0	15.5
58261	LomaPrieta	1.50	3.0	16.0	0.250	26.0	2.8	0.06	8.8	2.0	15.5
14533	Whittier	0.29	5.0	80.8	0.010	5.2	2.9	0.04	4.3	1.3	29.2
14533	Whittier	0.30	7.7	80.8	0.007	3.9	2.1	0.05	7.1	1.2	24.0
14654	Northridge	0.48	1.9	57.3	0.046	14.7	4.9	0.11	10.9	2.9	43.1
14654	Northridge	0.58	2.7	57.3	0.099	26.4	7.2	0.09	10.2	2.7	45.6
24288	Chinohills	0.31	3.2	107.1	0.004	2.1	1.1	0.07	6.5	1.0	18.0
24288	Chinohills	0.35	3.1	107.1	0.003	1.6	0.7	0.06	4.9	0.6	16.5
24569	Northridge	0.31	3.2	72.0	0.025	12.7	6.4	0.14	12.6	3.1	28.8
24569	Northridge	0.32	2.9	72.0	0.024	11.7	5.7	0.20	16.2	2.9	19.3
24602	Chinohills	0.17	1.1	218.3	0.001	1.3	1.2	0.09	8.2	1.1	9.3
24602	Landers	0.17	1.2	218.3	0.017	16.5	16.0	0.12	7.7	4.0	90.8
24602	Landers	0.17	1.4	218.3	0.020	17.9	16.7	0.10	9.3	10.4	82.4
24602	Northridge	0.16	1.3	218.3	0.012	11.1	10.8	0.13	9.2	4.2	33.4
24602	Northridge	0.17	1.1	218.3	0.005	4.2	3.9	0.18	14.5	2.4	18.4
24602	Sierra Madre	0.18	1.4	218.3	0.003	2.3	2.0	0.10	5.0	0.6	11.3
24629	Northridge	0.16	1.2	211.1	0.007	6.9	6.9	0.17	10.1	2.8	28.3
24629	Northridge	0.19	1.1	211.1	0.011	8.9	7.4	0.10	8.4	3.1	30.5
24629	Chinohills	0.16	2.9	211.1	0.001	1.2	1.2	0.06	5.8	0.9	14.6
24629	Chinohills	0.19	2.7	211.1	0.001	0.5	0.4	0.07	4.1	0.3	15.7
24643	Northridge	0.26	3.0	92.7	0.047	28.4	17.5	0.52	27.8	6.2	60.7
24643	Northridge	0.29	3.6	92.7	0.049	26.6	14.6	0.26	16.2	4.9	19.1
57318	AlumRock	0.45	2.0	83.8	0.021	7.3	2.6	0.06	6.1	1.2	16.8
57318	AlumRock	0.68	2.2	83.8	0.039	9.0	2.1	0.06	4.1	0.8	16.9
57357	LomaPrieta	0.45	1.3	64.2	0.212	73.0	25.6	0.09	23.1	9.3	37.7
57357	LomaPrieta	0.48	2.2	64.2	0.166	54.5	18.2	0.10	17.6	7.1	32.8
58354	LomaPrieta	0.75	2.1	61.3	0.039	8.1	1.7	0.08	6.8	0.8	15.1
58354	LomaPrieta	0.78	2.6	61.3	0.047	9.3	1.9	0.07	6.2	0.9	18.5

Station #	Earthquake	f ₁ (Hz)	ζ ₁ (%)	H(m)	S _A (g)	S _V (cm/s)	S _D (cm)	PGA(g)	PGV(cm/s)	PGD(cm)	t _{0.9} (s)
58480	LomaPrieta	0.31	5.0	69.9	0.035	17.5	8.9	0.14	16.5	4.9	11.5
58480	LomaPrieta	0.44	3.3	69.9	0.034	11.9	4.3	0.16	15.8	2.6	11.3
58532	LomaPrieta	0.16	1.7	172.0	0.014	13.7	13.5	0.20	26.4	7.9	13.7
58532	LomaPrieta	0.19	1.4	172.0	0.008	6.7	5.6	0.12	15.7	3.4	15.9
58262	LomaPrieta	3.66	3.3	7.2	0.195	8.3	0.4	0.11	12.8	2.4	12.4
58262	LomaPrieta	4.86	6.1	7.2	0.199	6.4	0.2	0.11	18.8	5.1	10.3
47391	MorganHill84	1.7	7	9.1	0.129	11.9	1.1	0.07	6.5	3.1	32.8
47391	MorganHill84	1.92	5.7	9.1	0.112	9.1	0.8	0.07	6.5	3.1	32.8
57502	LomaPrieta	4.26	8.3	9.6	0.299	10.9	0.4	0.11	28.0	19.7	34.6
57502	LomaPrieta	4.72	6.5	9.6	0.320	10.6	0.4	0.11	28.0	19.7	34.6
58348	LomaPrieta	2.22	8.2	12.4	0.222	15.6	1.1	0.12	20.0	5.8	16.0
58348	LomaPrieta	3.05	8.1	12.4	0.134	6.9	0.4	0.08	12.1	2.4	18.5
58348	Lafayette	2.4	6.7	12.4	0.063	4.1	0.3	0.06	2.1	0.2	7.6
58348	Lafayette	3.21	8.8	12.4	0.070	3.4	0.2	0.05	1.9	0.1	6.5
23511	Whittier	3.5	5.4	12.3	0.110	4.9	0.2	0.05	2.0	0.1	15.3
23511	Whittier	4.47	4.3	12.3	0.091	3.2	0.1	0.05	2.3	0.2	16.6
23511	Chinohills	2.98	6.6	12.3	0.232	12.2	0.7	0.13	11.9	2.3	8.0
23511	Chinohills	3.42	5.3	12.3	0.173	7.9	0.4	0.13	11.9	2.4	8.2
23495	BigBear	1.94	7.3	8.8	0.369	29.7	2.4	0.17	12.4	1.9	17.1
23495	PalmSprings	2.5	7.1	8.8	0.137	8.5	0.5	0.04	3.6	0.5	30.0
23495	PalmSprings	3.76	5.1	8.8	0.098	4.1	0.2	0.04	3.4	0.5	25.7
23495	SanBernardino	2.3	8.3	8.8	0.048	3.3	0.2	0.06	2.3	0.2	13.8
23495	SanBernardino	3.71	6.3	8.8	0.104	4.4	0.2	0.05	1.9	0.1	13.6
58503	LomaPrieta	3.48	6	11.4	0.204	9.2	0.4	0.10	14.5	2.3	10.3
58503	LomaPrieta	3.9	4.5	11.4	0.178	7.1	0.3	0.10	14.5	2.3	10.3
58503	Elcerrito	3.95	5.8	11.4	0.103	4.1	0.2	0.06	2.0	0.1	2.8
58503	Elcerrito	5.05	5.6	11.4	0.111	3.4	0.1	0.06	2.0	0.1	2.8
23622	Landers	4.17	7.1	5.6	0.164	6.2	0.2	0.09	14.4	8.1	35.4
23622	Landers	6.52	4.6	5.6	0.188	4.5	0.1	0.08	13.3	7.7	36.5
25213	SantaBarbara	3.12	5.5	10.1	1.043	52.2	2.7	0.38	34.3	5.5	7.3
58235	MorganHill84	4.07	6.1	10.1	0.201	7.7	0.3	0.06	4.2	0.9	21.9
58235	MorganHill84	4.3	4.3	10.1	0.190	6.9	0.3	0.06	4.2	0.9	21.9
58235	LomaPrieta	3.37	8.1	10.1	0.728	33.7	1.6	0.32	36.6	7.3	10.4
58235	LomaPrieta	3.82	6.2	10.1	0.561	22.9	1.0	0.24	37.0	6.4	11.0
58196	Lafayette	3	6.8	17.0	0.115	6.0	0.3	0.06	2.4	0.1	1.6
58196	Lafayette	5.64	8.4	17.0	0.120	3.3	0.1	0.06	3.1	0.2	1.7
58196	Piedmont	3	2.7	17.0	0.128	6.7	0.4	0.06	2.4	0.2	2.5
58196	Piedmont	5.12	6.3	17.0	0.183	5.6	0.2	0.07	2.9	0.2	2.1
58488	LomaPrieta	4	4.2	15.2	0.136	5.3	0.2	0.05	4.2	0.8	19.2
58488	LomaPrieta	4.5	4.2	15.2	0.116	4.0	0.1	0.05	4.2	0.8	19.2

Station #	Earthquake	f_1 (Hz)	ζ_1 (%)	H(m)	S_A (g)	S_V (cm/s)	S_D (cm)	PGA(g)	PGV(cm/s)	PGD(cm)	$t_{0.9}$ (s)
58462	LomaPrieta	1.04	5.4	25.9	0.106	15.9	2.4	0.10	10.4	2.0	25.5
58462	LomaPrieta	1.47	5.2	25.9	0.192	20.4	2.2	0.10	10.4	2.0	25.5
14311	Whittier	2.94	3	21.6	0.243	12.9	0.7	0.09	6.1	0.7	19.8
14311	Whittier	5.5	6.8	21.6	0.123	3.5	0.1	0.10	11.0	1.1	17.9
14311	Chinohills	3.02	2.3	21.6	0.087	4.5	0.2	0.07	7.7	1.4	26.3
14311	Chinohills	5.41	6.5	21.6	0.116	3.3	0.1	0.11	9.0	1.0	24.1
24463	Whittier	0.7	3.8	36.3	0.091	20.2	4.6	0.13	12.7	2.0	13.2
24463	Whittier	0.75	6.2	36.3	0.110	22.8	4.8	0.17	9.0	1.6	11.5
12284	BorregoSprings Jul2010	1.48	4.3	15.3	0.044	4.7	0.5	0.05	2.2	0.3	24.6
12284	BorregoSprings Jul2011	1.58	4.9	15.3	0.046	4.5	0.5	0.08	3.7	0.5	15.7
12284	Calexico Apr2010	1.45	4	15.3	0.104	11.2	1.2	0.05	4.3	3.2	37.0
12284	Calexico Apr2011	1.55	5.2	15.3	0.083	8.3	0.9	0.04	4.0	3.3	38.8
12284	PalmSprings	1.66	3.8	15.3	0.082	7.7	0.7	0.09	8.1	2.4	24.1
12284	PalmSprings	1.78	5.2	15.3	0.087	7.6	0.7	0.11	8.7	2.4	24.2
23285	SanBernardino	1.92	2.9	20.4	0.012	1.0	0.1	0.06	1.4	0.1	5.0
23285	SanBernardino	2.35	4.3	20.4	0.019	1.3	0.1	0.06	1.4	0.1	5.0
24468	Northridge	0.63	4	35.0	0.082	20.3	5.1	0.12	8.7	1.4	17.4
24468	Northridge	0.65	3.9	35.0	0.086	20.6	5.0	0.12	8.7	1.4	17.4
24468	Whittier	0.65	5.2	35.0	0.110	26.3	6.4	0.32	20.1	2.4	6.3
24468	Whittier	0.69	2.8	35.0	0.137	31.2	7.2	0.32	20.1	2.4	6.3
24579	Landers	0.7	5.8	39.0	0.053	11.8	2.7	0.04	6.8	4.1	65.7
24579	Landers	0.81	5.3	39.0	0.064	12.4	2.4	0.04	6.8	4.1	65.7
24579	Northridge	0.66	6.9	39.0	0.092	21.7	5.2	0.15	13.4	2.9	21.2
24579	Northridge	0.76	6.8	39.0	0.116	23.8	5.0	0.15	13.4	2.9	21.2
47459	LomaPrieta	2.83	5.5	20.2	0.953	52.6	3.0	0.36	54.9	18.2	8.8
47459	LomaPrieta	3.93	6.7	20.2	0.453	18.0	0.7	0.27	33.3	9.0	11.8
58479	LomaPrieta	2.96	4.2	19.8	0.164	8.7	0.5	0.07	15.1	4.2	8.9
58479	LomaPrieta	4.81	6.3	19.8	0.130	4.2	0.1	0.08	12.8	3.0	8.0
58490	LomaPrieta	1	4.5	23.8	0.216	33.6	5.4	0.11	16.2	2.7	14.9
58490	LomaPrieta	1.23	7.5	23.8	0.174	22.1	2.9	0.14	14.6	3.5	15.6
24655	Northridge	1.94	5.5	20.4	0.441	35.5	2.9	0.29	19.1	4.4	15.2
24571	Landers	0.5	4.1	41.5	0.044	13.8	4.4	0.04	6.4	2.0	30.5
24571	Landers	0.78	4.1	41.5	0.125	25.1	5.1	0.05	6.2	1.8	31.5
24571	Northridge	0.47	4.1	41.5	0.024	8.1	2.7	0.16	8.9	1.3	12.0
24571	Northridge	0.77	2.9	41.5	0.072	14.6	3.0	0.18	10.0	0.8	10.5
24571	SierraMadre	0.51	5	41.5	0.030	9.0	2.8	0.10	7.5	0.8	7.6
58394	LomaPrieta	0.58	4.4	31.7	0.136	36.5	10.0	0.12	15.0	3.3	14.4
58394	LomaPrieta	0.82	4.3	31.7	0.108	20.5	4.0	0.11	15.6	2.8	12.7

Station #	Earthquake	f_1 (Hz)	ζ_1 (%)	H(m)	S_A (g)	S_V (cm/s)	S_D (cm)	PGA(g)	PGV(cm/s)	PGD(cm)	$t_{0.9}$ (s)
24385	SierraMadre	1.86	5.9	26.8	0.103	8.7	0.7	0.07	4.6	0.7	11.7
24385	SierraMadre	2.1	3.3	26.8	0.245	18.2	1.4	0.11	8.5	0.9	9.4
24385	Whittier	1.82	9.3	26.8	0.241	20.7	1.8	0.21	11.0	1.0	6.3
24385	Whittier	2.22	9.4	26.8	0.204	14.4	1.0	0.20	8.6	1.1	7.1
57355	MorganHill84	1.1	3.6	37.8	0.144	20.5	3.0	0.06	12.3	3.4	23.2
57355	MorganHill84	1.6	3.7	37.8	0.158	15.4	1.5	0.06	10.4	2.5	26.9
57355	AlumRock	0.96	3.4	37.8	0.063	10.3	1.7	0.07	5.8	1.1	17.9
57355	AlumRock	1.44	3.6	37.8	0.044	4.7	0.5	0.06	3.6	0.4	13.6
57355	LomaPrieta	0.99	3.6	37.8	0.133	20.9	3.4	0.09	18.1	9.9	25.6
57355	LomaPrieta	1.34	6.3	37.8	0.296	34.4	4.1	0.10	22.0	12.9	24.2
57356	MorganHill84	1.65	3.8	29.3	0.139	13.2	1.3	0.05	12.1	2.8	27.0
57356	MorganHill84	2.3	5	29.3	0.114	7.7	0.5	0.06	7.4	2.2	27.1
57356	LomaPrieta	1.49	6	29.3	0.185	19.4	2.1	0.09	16.5	7.3	17.6
57356	LomaPrieta	2.29	6	29.3	0.197	13.4	0.9	0.11	20.2	11.4	19.9
57356	AlumRock	1.37	3.8	29.3	0.088	10.0	1.2	0.11	8.0	1.1	10.7
57356	AlumRock	2.3	3.6	29.3	0.088	6.0	0.4	0.08	3.2	0.6	16.1
24322	Northridge	0.32	3	50.0	0.064	31.4	15.6	0.83	60.7	13.5	8.6
24322	Northridge	0.34	5.9	50.0	0.112	51.5	24.1	0.37	29.7	8.1	16.4
24322	Whittier	0.4	3.1	50.0	0.008	3.3	1.3	0.26	8.1	0.5	11.3
24322	Whittier	0.45	4.5	50.0	0.013	4.3	1.5	0.17	11.5	1.0	10.3
24322	Chinohills	0.65	2.2	50.0	0.015	3.7	0.9	0.07	3.4	0.3	14.7
24322	Chinohills	0.67	3.6	50.0	0.011	2.6	0.6	0.04	2.4	0.2	24.5
58364	LomaPrieta	1.25	3.5	39.2	0.103	12.9	1.6	0.05	7.6	1.4	18.7
58364	LomaPrieta	1.6	3.1	39.2	0.168	16.4	1.6	0.06	8.7	1.6	18.7
14578	Chinohills	0.8	5.5	35.4	0.050	9.7	1.9	0.10	9.1	1.0	18.9
14578	Chinohills	0.9	6.4	35.4	0.099	17.2	3.0	0.14	12.5	2.0	17.5
14578	Northridge	0.84	5	35.4	0.034	6.3	1.2	0.07	5.5	1.4	42.1
14578	Northridge	0.93	7.5	35.4	0.057	9.6	1.6	0.11	6.7	1.5	36.9
24601	Northridge	0.86	4.2	42.3	0.029	5.2	1.0	0.02	1.7	0.6	66.7
24601	Northridge	0.94	4	42.3	0.042	7.1	1.2	0.05	3.8	1.0	51.8
24601	SierraMadre	0.99	2.5	42.3	0.068	10.7	1.7	0.07	5.2	0.7	13.1
24601	SierraMadre	1.2	6.5	42.3	0.071	9.2	1.2	0.06	4.4	1.0	15.5
24601	Landers	0.94	3.2	42.3	0.102	16.9	2.9	0.04	7.3	6.5	57.1
24601	Landers	1.16	5.8	42.3	0.076	10.2	1.4	0.04	11.6	7.6	55.1
24581	Chinohills	0.56	8.5	47.3	0.010	2.7	0.8	0.06	4.1	0.4	13.3
24581	Chinohills	1.03	6.2	47.3	0.065	9.8	1.5	0.07	5.9	1.0	13.4
24236	Whittier	0.54	7.5	42.1	0.041	12.0	3.5	0.12	9.5	1.4	13.0
24236	Whittier	1.63	9.2	42.1	0.114	10.9	1.1	0.06	6.3	0.9	15.2
58483	LomaPrieta	0.41	3.3	66.8	0.057	21.7	8.4	0.12	17.1	4.3	13.9
58483	LomaPrieta	0.5	6.6	66.8	0.075	23.3	7.4	0.12	17.1	4.3	13.9

Station #	Earthquake	f_1 (Hz)	ζ_1 (%)	H(m)	SA(g)	SV(cm/s)	SD(cm)	PGA(g)	PGV(cm/s)	PGD(cm)	$t_{0.9}$ (s)
13589	Landers	1.22	4.5	44.8	0.124	15.9	2.1	0.04	6.3	2.8	68.6
13589	Landers	1.41	3.7	44.8	0.118	13.1	1.5	0.05	12.3	6.8	42.1
13589	Northridge	1.18	4.2	44.8	0.092	12.2	1.6	0.08	5.6	1.7	50.7
13589	Northridge	1.36	3.7	44.8	0.107	12.3	1.4	0.05	5.8	1.4	58.5
58639	Piedmont	1.24	4.1	34.8	0.012	1.5	0.2	0.03	1.5	0.1	4.6
58639	Piedmont	1.81	2.9	34.8	0.021	1.8	0.2	0.06	2.3	0.1	4.0
24680	Chinohills	0.68	4.6	49.1	0.011	2.6	0.6	0.03	2.0	0.3	32.6
24680	Chinohills	0.85	3.8	49.1	0.018	3.3	0.6	0.05	2.7	0.3	25.8
12266	Anza	3.71	12.0	7.9	0.255	10.7	0.5	0.08	2.5	0.1	9.8
12266	Anza	5.97	3.9	7.9	0.185	4.8	0.1	0.08	2.5	0.1	9.8
14606	Northridge	1.45	5.4	23.2	0.093	10.0	1.1	0.11	8.6	1.6	16.6
14606	Northridge	1.58	7.0	23.2	0.225	22.3	2.2	0.16	12.0	1.5	13.5
14606	Chinohills	1.64	5.4	23.2	0.146	13.9	1.4	0.10	6.3	0.4	9.5
14606	Chinohills	1.85	6.0	23.2	0.276	23.3	2.0	0.13	11.9	1.8	7.6
14606	WhittierNarrows	1.68	5.7	23.2	0.027	2.5	0.2	0.15	4.8	0.2	1.6
14606	WhittierNarrows	2.03	4.7	23.2	0.035	2.7	0.2	0.22	6.1	0.2	0.8
24517	Landers	1.60	7.0	12.7	0.120	11.7	1.2	0.05	7.1	3.2	41.2
24517	Landers	2.86	5.7	12.7	0.150	8.2	0.5	0.05	7.1	3.2	41.2
24517	Northridge	1.65	10.1	12.7	0.172	16.3	1.6	0.06	9.3	2.5	27.4
24517	Northridge	2.25	9.8	12.7	0.174	12.1	0.9	0.06	9.3	2.5	27.4
24517	Whittier	2.49	3.0	12.7	0.133	8.3	0.5	0.05	2.8	0.2	11.6
24517	Whittier	3.35	6.5	12.7	0.151	7.1	0.3	0.05	2.8	0.2	11.6
57476	LomaPrieta	0.75	8.8	7.9	0.440	92.0	19.6	0.29	6.5	0.3	8.2
57476	LomaPrieta	1.16	9.6	7.9	0.261	35.1	4.8	0.24	0.7	0.1	12.2
58264	LomaPrieta	3.7	9.8	7.3	0.477	20.1	0.9	0.21	33.7	14.2	27.4
58492	LomaPrieta	1.37	6.3	22.8	0.195	22.2	2.6	0.06	7.8	2.1	18.4
89473	Petrolia	2.72	3.2	6.7	0.211	12.1	0.7	0.13	17.8	4.4	18.8
89473	Petrolia	3.22	2.3	6.7	0.204	9.9	0.5	0.13	17.8	4.4	18.8
89473	Ferndale Jan2010	3.3	12.5	6.7	0.371	17.6	0.8	0.14	11.8	2.1	17.2
89473	Ferndale Jan2011	4.2	11.2	6.7	0.314	11.7	0.4	0.14	11.8	2.1	17.2
89473	PetroliaAftershock	2.77	2.6	6.7	0.440	24.8	1.4	0.16	12.5	2.3	13.0
89473	PetroliaAftershock	3.08	4.6	6.7	0.490	24.8	1.3	0.16	12.5	2.3	13.0
89494	Ferndale Jan2010	2.93	12.7	13.6	0.562	29.9	1.6	0.22	22.4	5.2	15.3
89494	Ferndale Jan2011	3.28	8.6	13.6	0.570	27.1	1.3	0.22	22.4	5.2	15.3
12759	Anza	4.61	5.3	3.8	0.478	16.2	0.6	0.22	10.9	0.9	8.2
12759	Anza	5.89	9.5	3.8	0.433	11.5	0.3	0.22	10.9	0.9	8.2
12759	BorregoSprings Jul2010	4.44	6.4	3.8	0.164	5.8	0.2	0.07	4.4	0.8	18.3
12759	BorregoSprings Jul2011	5.09	4.3	3.8	0.156	4.8	0.1	0.07	4.4	0.8	18.3
36695	SanSimeon	4.74	12.7	5.0	1.161	38.2	1.3	0.45	30.1	7.3	9.9
36695	SanSimeon	4.94	8.8	5.0	1.279	40.4	1.3	0.45	30.1	7.3	9.9

Station #	Earthquake	f_1 (Hz)	ζ_1 (%)	H(m)	S_A (g)	S_V (cm/s)	S_D (cm)	PGA(g)	PGV(cm/s)	PGD(cm)	$t_{0.9}$ (s)
36695	Atascadero	5.50	5.9	5.0	0.090	2.5	0.1	0.06	1.4	0.0	3.8
36695	Atascadero	5.60	2.8	5.0	0.091	2.5	0.1	0.06	1.4	0.0	3.8
89687	Ferndale Jan2010	2.73	7.7	7.9	0.570	32.6	1.9	0.25	26.1	5.3	9.8
89687	Ferndale Jan2011	3.28	8.7	7.9	0.528	25.1	1.2	0.25	26.1	5.3	9.8

References

Bernal, D. (2007). Optimal Discrete to Continuous Transfer for Band Limited Inputs. *Journal of Engineering Mechanics* 133(12), 1370-1377.

Casella, G. and Berger, R. (2001). *Statistical Inference*, Duxbury Press.

Gersch, W. (1974). On the achievable accuracy of structural system parameter estimates. *Journal of Sound and Vibration* 34(1), 63–79.

Hart, G.C. & Vasudevan R. (1975). Earthquake design of buildings: damping. *ASCE Journal of the Structural Division* 101(1), 11–29.

Heylen, W. Lammens, S. & Sas, P. (1997). *Modal Analysis Theory and Testing*. Katholieke Universiteit Leuven, Departement Werktuigkunde.

Jeary, A. P. (1986). Damping in tall buildings—A mechanism and a predictor. *Earthquake Engineering & Structural Dynamics* 14(5), 733–750.

Juang, J. (1994). *Applied System Identification*. Englewood Cliffs, NJ: PTR Prentice Hall, Inc.

Lagomarsino, S. (1993). Forecast models for damping and vibration periods of buildings. *Journal of Wind Engineering and Industrial Aerodynamics* 48(2), 221–239.

McVerry, G.H. (1979). Frequency Domain Identification of Structural Models from Earthquake Records. *Ph.D. thesis, California Institute of Technology*.

McVerry, G.H. (1980). Structural identification in the frequency domain from earthquake records. *Earthquake Engineering and Structural Dynamics* 8(2), 161–80.

Sasaki, A., Suganuma, S., Suda, K. & Tamura, Y. (1998). *Proc., Annual Meeting of the Architectural Institute of Japan (AIJ), Fukuoka, AIJ Japan, B-2, 379–380*.

Satake, N., Suda, K. I., Arakawa, T., Sasaki, A., & Tamura, Y. (2003). Damping evaluation using full scale data of buildings in Japan. *Journal of Structural Engineering* 129(4), 470-477.

Tamura, Y. & Suganuma, S. (1996). Evaluation of amplitude dependent damping and natural frequency of buildings during strong winds. *Journal of Wind Engineering and Industrial Aerodynamics* 59(2), 115-130.

van den Bos, A. (2007). *Parameter Estimation for Scientists and Engineers*, Wiley Interscience.

Van Overschee, P., & De Moor, B. (1996). Subspace identification for linear systems: Theory, implementation, applications. *Kluwer Academic, Boston*.

Verhaegen, M. & Verdult V. (2007). *Filtering and System Identification: an Introduction*. Cambridge University Press.

Zhang, Z. & Cho, C. (2009). Experimental Study on Damping Ratios of in-situ Buildings. *World Academy of Science, Engineering and Technology* 26, 614-618.